Stability of Spin-Orbit Coupled Fermi Gases with Population Imbalance

M. Iskin[1] and A. L. Subaşı[2]

[1]Department of Physics, Koç University, Rumelifeneri Yolu, 34450 Sarıyer, Istanbul, Turkey
[2]Department of Physics, Faculty of Science and Letters, Istanbul Technical University, 34469 Maslak, Istanbul, Turkey

(Received 2 June 2011; published 28 July 2011)

We use the self-consistent mean-field theory to analyze the effects of Rashba-type spin-orbit coupling (SOC) on the ground-state phase diagram of population-imbalanced Fermi gases throughout the BCS–Bose-Einstein condensate evolution. We find that the SOC and population imbalance are counteracting, and that this competition tends to stabilize the uniform superfluid phase against the phase separation. However, we also show that the SOC stabilizes (destabilizes) the uniform superfluid phase against the normal phase for low (high) population imbalances. In addition, we find topological quantum phase transitions associated with the appearance of momentum-space regions with zero quasiparticle energies, and study their signatures in the momentum distribution.

DOI: 10.1103/PhysRevLett.107.050402 PACS numbers: 05.30.Fk, 03.75.Hh, 03.75.Ss

Introduction.—The recent realization of synthetic gauge fields with neutral bosonic atoms [1], evidently seen from the appearance of vortices in a Bose-Einstein condensate (BEC), has sparked a new wave of theoretical interest in the cold atom community. This novel technique uses a spatially dependent optical coupling between internal states of the atoms, and can be used to engineer more complicated gauge fields by dressing two atomic spin states with a pair of lasers. For instance, it has recently been used to create and study the effects of spin-orbit coupling (SOC) in a neutral atomic BEC with equal Rashba and Dresselhaus strengths [2]. Since this method is equally applicable for neutral fermionic atoms, and given that the coupling between a quantum particle's spin and its momentum is crucial for the topological insulators and quantum spin Hall states, which have recently received immense interest in the condensed matter community [3], it may allow for the realization of topologically nontrivial states in atomic systems with possibly a broad interest in the physics community [4–6].

Motivated by the recent success in realization of the SOC Bose gases [2], and by a practical proposal for generating a SOC in ^{40}K atoms [7], effects of the SOC have recently been studied for the two-component Fermi gases: (i) the two-body problem exactly [8], and (ii) the many-body problem in the BCS mean-field approximation [5,6,9–11]. It has been found that the increased density of states due to the SOC plays a crucial role for both problems. In particular, for the two-body problem, this gives rise to a two-body bound state even on the BCS side ($a_s < 0$) of a resonance [8]. For the many-body problem, the increased density of states favors the pairing so significantly that increasing the SOC, while the scattering length is held fixed, eventually induces a BCS-BEC crossover even for a weakly interacting system when $a_s \to 0^-$ [9–11]. In addition, the SOC leads to an anisotropic superfluid, the signatures of which could be observed in the momentum distribution or the single-particle spectral function for sufficiently strong SOCs [11].

In this Letter, we study the competition between the SOC and population imbalance on the ground-state phase diagram of two-component Fermi gases across a Feshbach resonance, i.e., throughout the BCS-BEC evolution. Our main results are shown in Fig. 1, and they are as follows. In the absence of a SOC, the phase diagram of population-imbalanced mixtures is well studied in the literature [12], and it mainly involves normal (N), phase separation (PS), and topologically distinct gapless superfluid (GSF) as well as the trivial gapped superfluid (SF) phases. In particular, at and around unitarity ($|a_s| \to \infty$), the system changes from

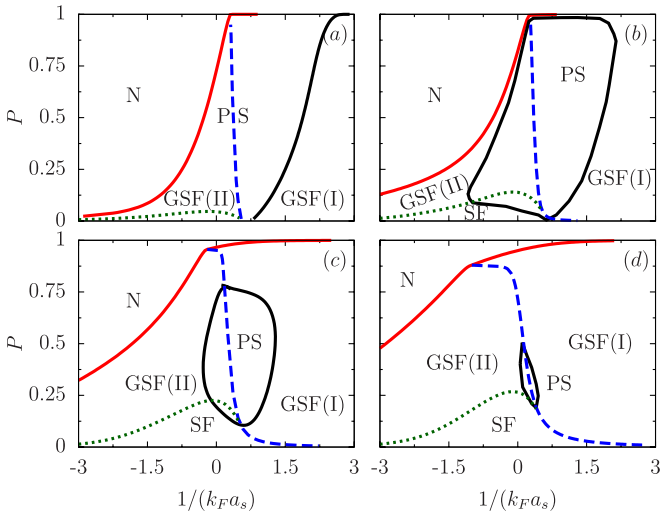

FIG. 1 (color online). The ground-state phase diagrams are shown as a function of population imbalance $P = (N_\uparrow - N_\downarrow)/N$ and scattering parameter $1/(k_F a_s)$, where the SOC parameter $m\alpha/k_F$ is set to 0.005 in (a), 0.05 in (b), 0.15 in (c), and 0.25 in (d). We show normal (N), phase separation (PS), gapped superfluid (SF), and gapless superfluid (GSF) phases, where the dashed blue and dotted green lines separate topologically distinct regions.

SF to PS and then to N as a function of increasing population imbalance. In this Letter, we show that the SOC and population imbalance are counteracting, and that this competition always tends to stabilize the GSF phase against the PS. However, we also show that the SOC stabilizes (destabilizes) the GSF phase against the N phase for low (high) population imbalances. In addition, since the SOC stabilizes the GSF phase for a very large parameter region, where most experiments are conducted [13], it may allow for a possible realization of the GSF phase with cold atoms.

Mean-field Hamiltonian.—To obtain these results, we use the mean-field Hamiltonian [6,14] (in units of $\hbar = 1 = k_B$)

$$H = \frac{1}{2}\sum_{\mathbf{k}} \psi_{\mathbf{k}}^{\dagger} \begin{pmatrix} \xi_{\mathbf{k},\uparrow} & S_{\mathbf{k}} & 0 & \Delta \\ S_{\mathbf{k}}^{*} & \xi_{\mathbf{k},\downarrow} & -\Delta & 0 \\ 0 & -\Delta^{*} & -\xi_{-\mathbf{k},\uparrow} & -S_{-\mathbf{k}}^{*} \\ \Delta^{*} & 0 & -S_{-\mathbf{k}} & -\xi_{-\mathbf{k},\downarrow} \end{pmatrix} \psi_{\mathbf{k}}, \quad (1)$$

which is defined up to the constant $C = (1/2)\sum_{\mathbf{k},\sigma}\xi_{\mathbf{k},\sigma} + |\Delta|^2/g$. Here, $\psi_{\mathbf{k}}^{\dagger} = [a_{\mathbf{k},\uparrow}^{\dagger}, a_{\mathbf{k},\downarrow}^{\dagger}, a_{-\mathbf{k},\uparrow}, a_{-\mathbf{k},\downarrow}]$ denotes the fermionic operators collectively, where $a_{\mathbf{k},\sigma}^{\dagger}$ ($a_{\mathbf{k},\sigma}$) creates (annihilates) a spin-σ fermion with momentum $\mathbf{k}$, $\xi_{\mathbf{k},\sigma} = \xi_{-\mathbf{k},\sigma} = \epsilon_{\mathbf{k},\sigma} - \mu_{\sigma}$ has the inversion symmetry with $\epsilon_{\mathbf{k},\sigma} = k^2/(2m_{\sigma})$ the kinetic energy, μ_{σ} the chemical potential, and $k = \sqrt{k_x^2 + k_y^2 + k_z^2}$. Here, $\Delta = g\langle a_{\mathbf{k},\uparrow} a_{-\mathbf{k},\downarrow}\rangle$ is the mean-field order parameter, where $g \geq 0$ is the strength of the attractive particle-particle interaction which is assumed to be local, and $\langle\cdots\rangle$ is a thermal average. We consider only a Rashba-type SOC, i.e., $S_{\mathbf{k}} = -S_{-\mathbf{k}} = \alpha(k_y - ik_x)$, where $\alpha \geq 0$ is its strength.

Self-consistency equations.—Following the usual procedure, i.e., $\partial\Omega/\partial|\Delta| = 0$ for the order parameter and $N_{\uparrow} + sN_{\downarrow} = -\partial\Omega/\partial\mu_s$ for the number equations where Ω is the mean-field thermodynamic potential, $s = \pm$ and $\mu_s = (\mu_{\uparrow} + s\mu_{\downarrow})/2$, we obtain the self-consistency equations

$$\frac{2|\Delta|}{g} = \frac{1}{2}\sum_{\mathbf{k},s} \frac{\partial E_{\mathbf{k},s}}{\partial|\Delta|} \tanh\left(\frac{E_{\mathbf{k},s}}{2T}\right), \quad (2)$$

$$N_{\uparrow} \pm N_{\downarrow} = \frac{1}{2}\sum_{\mathbf{k},s}\left[\frac{1 \pm 1}{2} + \frac{\partial E_{\mathbf{k},s}}{\partial\mu_{\pm}} \tanh\left(\frac{E_{\mathbf{k},s}}{2T}\right)\right]. \quad (3)$$

Here, T is the temperature and $E_{\mathbf{k},s}^2 = \xi_{\mathbf{k},+}^2 + \xi_{\mathbf{k},-}^2 + |\Delta|^2 + |S_{\mathbf{k}}|^2 + 2sA_{\mathbf{k}}$ gives the quasiparticle excitation spectrum [5,6], where $A_{\mathbf{k}} = \sqrt{\xi_{\mathbf{k},-}^2(\xi_{\mathbf{k},+}^2 + |\Delta|^2) + |S_{\mathbf{k}}|^2\xi_{\mathbf{k},+}^2}$, $\xi_{\mathbf{k},s} = \epsilon_{\mathbf{k},s} - \mu_s$ with $\epsilon_{\mathbf{k},s} = (\epsilon_{\mathbf{k},\uparrow} + s\epsilon_{\mathbf{k},\downarrow})/2 = k^2/(2m_s)$ and $m_s = 2m_{\uparrow}m_{\downarrow}/(m_{\downarrow} + sm_{\uparrow})$. Note that m_+ is twice the reduced mass of $\uparrow$ and $\downarrow$ particles, and $m_- \to \infty$ for mass-balanced ($m_{\uparrow} = m_{\downarrow}$) mixtures. In Eqs. (2) and (3), the derivatives of the quasiparticle energies are given by $\partial E_{\mathbf{k},s}/\partial|\Delta| = (1 + s\xi_{\mathbf{k},-}^2/A_{\mathbf{k}})|\Delta|/E_{\mathbf{k},s}$ for the order parameter, $\partial E_{\mathbf{k},s}/\partial\mu_+ = -[1 + s(\xi_{\mathbf{k},-}^2 + |S_{\mathbf{k}}|^2)/A_{\mathbf{k}}]\xi_{\mathbf{k},-}/E_{\mathbf{k},s}$ for the average chemical potential, and $\partial E_{\mathbf{k},s}/\partial\mu_- = -[1 + s(\xi_{\mathbf{k},+}^2 + |\Delta|^2)/A_{\mathbf{k}}]\xi_{\mathbf{k},-}/E_{\mathbf{k},s}$ for the half of the chemical potential difference.

Equations (2) and (3) are the generalization of the mean-field expressions to the case of population- and/or mass-imbalanced mixtures, and they recover the known expressions (a) when $\xi_{\mathbf{k},-} = 0$ for which $E_{\mathbf{k},s}$ simplifies to $E_{\mathbf{k},s}^2 = (\xi_{\mathbf{k},+} + s|S_{\mathbf{k}}|)^2 + |\Delta|^2$, and (b) when $|S_{\mathbf{k}}| = 0$ for which $E_{\mathbf{k},s}$ simplifies to $E_{\mathbf{k},s}^2 = [s\xi_{\mathbf{k},-} + \sqrt{\xi_{\mathbf{k},+}^2 + |\Delta|^2}]^2$. We eliminate the theoretical parameter g in favor of the experimentally relevant s-wave scattering length a_s via the relation, $1/g = -m_+V/(4\pi a_s) + \sum_{\mathbf{k}} 1/(2\epsilon_{\mathbf{k},+})$, where V is the volume. g can also be eliminated in favor of the two-body binding energy $\epsilon_b \leq 0$ in vacuum via the relation [8] $1/g = (1/2)\sum_{\mathbf{k},s} 1/(2\varepsilon_{\mathbf{k},s} + \epsilon_{\mathrm{th}} - \epsilon_b)$, where $\varepsilon_{\mathbf{k},s} = \epsilon_{\mathbf{k},+} + s\sqrt{\epsilon_{\mathbf{k},-}^2 + |S_{\mathbf{k}}|^2}$ is the single-particle noninteracting dispersion in the helicity basis, and ϵ_{th} is the threshold for the two-body scattering. For the Rashba-type SOC, and assuming $m_{\uparrow} \leq m_{\downarrow}$, we obtain $\epsilon_{\mathrm{th}} = 2\alpha^2 m_-(m_- - \sqrt{m_-^2 - m_+^2})/m_+$, which gives $\epsilon_{\mathrm{th}} = m_+\alpha^2$ when $m_- \gg m_+$, i.e., $m_{\uparrow} \lesssim m_{\downarrow}$.

Thermodynamic stability.—To construct the phase diagram, we solve the self-consistency equations and check the stability of these solutions for the uniform superfluid phase using the compressibility (or the curvature) criterion [15,16]. This says that the compressibility matrix $\kappa(T)$ with elements $\kappa_{\sigma,\sigma'}(T) = -\partial^2\Omega/(\partial\mu_{\sigma}\partial\mu_{\sigma'})$ needs to be positive definite, and it is directly related to the condition that the curvature of Ω with respect to $|\Delta|$, i.e.,

$$\frac{\partial^2\Omega}{\partial|\Delta|^2} = \frac{1}{2}\sum_{\mathbf{k},s}\left\{-\frac{1}{4T}\left(\frac{\partial E_{\mathbf{k},s}}{\partial|\Delta|}\right)^2 \mathrm{sech}^2\left(\frac{E_{\mathbf{k},s}}{2T}\right) + \left[s\frac{|\Delta|^2\xi_{\mathbf{k},-}^4}{A_{\mathbf{k}}^3} + \left(\frac{\partial E_{\mathbf{k},s}}{\partial|\Delta|}\right)^2\right]\frac{\tanh\left(\frac{E_{\mathbf{k},s}}{2T}\right)}{2E_{\mathbf{k},s}}\right\}, \quad (4)$$

needs to be positive. When at least one of the eigenvalues of $\kappa(T)$, or the curvature $\partial^2\Omega/\partial|\Delta|^2$ is negative, the uniform mean-field solution does not correspond to a minimum of Ω, and a nonuniform superfluid phase, e.g., a phase separation, is favored [15,16].

Rashba-type SOC for mass- and population-balanced mixtures.—To get more insight into the effects of the SOC in the BCS-BEC evolution, let us first consider mass- and population-balanced ($m_{\sigma} = m$ and $N_{\sigma} = N/2$) mixtures, where N is the total number of fermions. This case is analytically more tractable, since the single-particle energy in the helicity basis simplifies to [14] $\varepsilon_{\mathbf{k},s} = k^2/(2m) + s\alpha k_{\perp}$, where $k_{\perp} = \sqrt{k_x^2 + k_y^2}$. For instance, the bound-state equation can be solved to obtain $1/a_s = \sqrt{m^2\alpha^2 - m\epsilon_b} + m\alpha\ln[\sqrt{-m\epsilon_b}/(\sqrt{m^2\alpha^2 - m\epsilon_b} + m\alpha)]$. In the weak SOC limit, when $m\alpha^2 \ll \epsilon_b$, this expression

gives $\epsilon_b \approx -1/(ma_s^2) + m\alpha^2$, up to the leading order in α, which recovers the usual result in the $\alpha \to 0$ limit. However, in the strong SOC limit, when $m\alpha^2 \gg \epsilon_b$, the general expression gives $\epsilon_b \approx -(4m\alpha^2/e^2)e^{-2/(m\alpha a_s)}$, which implies that a bound state exists even for $a_s < 0$, although its energy is exponentially small [8]. This is a result of increased density of states $D_s(\epsilon) = \sum_{\mathbf{k}} \delta(\epsilon - \varepsilon_{\mathbf{k},s})$ due to the SOC [8], where $\delta(x)$ is the Dirac-delta function.

In the case of noninteracting ($g = 0$ or $a_s \to 0^-$) mass- and population-balanced Fermi gases at zero temperature ($T = 0$), where $\mu_\sigma = \mu$, calculating the total number $N = N_+ + N_- = k_F^3 V/(3\pi^2)$ of fermions, where $N_s = \sum_{\mathbf{k}} \theta(\mu - \varepsilon_{\mathbf{k},s})$, we obtain $\mu \approx \epsilon_F - 3m\alpha^2/2$ up to the leading order in α when $m\alpha^2 \ll \epsilon_F$, and $\mu = -m\alpha^2/2 + 2k_F^3/(3\pi m^2 \alpha)$ when $\mu < 0$. Note that we conveniently choose the energy (length) scale as the Fermi energy ϵ_F (momentum k_F) of the $N_\sigma = N/2$ fermions.

It has been shown that increasing the SOC for a noninteracting Fermi gas leads to a change in the Fermi surface topology, when the number of fermions in the $+$-helicity band (N_+) vanishes [9]. This occurs when μ goes below the bottom of the energy band, i.e., $\mu = 0$, or when α increases beyond $\alpha = [4/(3\pi)]^{1/3} k_F/m \approx 0.75 k_F/m$. In some ways, this is similar to the usual BCS-BEC crossover problem, where the quasiparticle excitation spectrum changes behavior as a function of increasing the scattering parameter $1/(k_F a_s)$ at $\mu = 0$; i.e., its minimum is located at a finite (zero) momenta when $\mu > 0$ ($\mu < 0$). However, the topological transition discussed here is driven by increasing the SOC parameter α, and the origin of it can also be traced back to the change in the quasiparticle excitation spectrum when g is finite. For instance, for mass- and population-balanced mixtures, the excitation spectrum simplifies to [9–11,14] $E_{\mathbf{k},s} = \sqrt{(\varepsilon_{\mathbf{k},s} - \mu)^2 + |\Delta|^2}$, and it also has a change of behavior at $\mu = 0$. Having set up the formalism, we are now ready to discuss the competition between normal fluidity, uniform superfluidity, and phase separation across a Feshbach resonance.

Ground-state phase diagrams.—In the absence of a SOC and at low T, it is well established that the self-consistent solutions of Eqs. (2) and (3) are sufficient to describe the physics of fermion mixtures both in the BCS and the BEC limits, and that these equations also capture qualitatively the correct physics in the entire BCS-BEC evolution [12,15]. Hoping that the mean-field formalism remains sufficient in the presence of a SOC, here we analyze only the ground-state phase diagram of population-imbalanced but mass-balanced mixtures as a function of both the SOC and scattering parameters.

There are typically three phases in our phase diagrams. While the normal (N) phase is characterized by $\Delta = 0$, the uniform superfluid and nonuniform superfluid, e.g., phase separation (PS), are characterized by $\partial^2\Omega/\partial|\Delta|^2 > 0$ and $\partial^2\Omega/\partial|\Delta|^2 < 0$, respectively, when $\Delta \neq 0$. Furthermore, in addition to the topologically trivial gapped superfluid, the GSF phase can also be distinguished by two topologically distinct regions, depending on the momentum-space topology of their quasiparticle excitation spectrum (see below).

In Fig. 1, the phase diagrams are shown as a function of population imbalance $P = (N_\uparrow - N_\downarrow)/N$ and scattering parameter $1/(k_F a_s)$ for four different α values. Comparing these results with the $\alpha \to 0$ limit [15], it is clearly seen that the SOC and population imbalance are counteracting. On one hand, this competition always tends to stabilize the GSF phase against the PS, and therefore, at any given P, the system eventually becomes a GSF by increasing α, no matter how small $1/(k_F a_s)$ is. This is best seen in Fig. 2, where the phase diagrams are shown as a function of P and α for four different $1/(k_F a_s)$ values. On the other hand, we find that while the SOC stabilizes the GSF phase against the N phase for low P due to increased density of states, it destabilizes the GSF phase against the N phase for high P.

In both figures, the dashed blue and dotted green lines are obtained from the conditions $|\Delta|^2 = -\mu_\uparrow\mu_\downarrow$ and $|\Delta| = |\mu_-|$ (see below), respectively, and they separate the topologically distinct regions. As can be inferred from Fig. 2, the dashed blue line makes a dip as $1/(k_F a_s) \lesssim 0$, tip of which eventually touches the $P = 0$ line at $\alpha \approx 0.75 k_F/m$, consistent with our analysis above for the topological transition of a noninteracting ($a_s \to 0^-$) system. In Figs. 1 and 2, we also show that the SOC stabilizes the GSF for a very large parameter region, at and around the unitarity, which is normally unstable against PS when $\alpha = 0$, allowing for a possible realization with cold atoms, as discussed next in great detail.

Topological phase transition.—When $\alpha \to 0$, population imbalance is achieved when either $E_{\mathbf{k},+}$ (for $N_\downarrow > N_\uparrow$) or $E_{\mathbf{k},-}$ (for $N_\uparrow > N_\downarrow$) has zeros in some places of $\mathbf{k}$ space. Let us assume $N_\uparrow \geq N_\downarrow$ without losing generality,

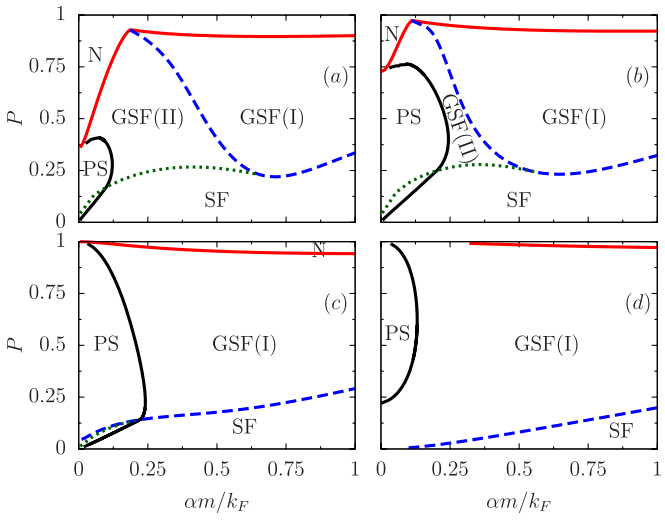

FIG. 2 (color online). The ground-state phase diagrams are shown as a function of $P = (N_\uparrow - N_\downarrow)/N$ and α, where $1/(k_F a_s)$ is set to -0.5 in (a), 0 in (b), 0.5 in (c), and 1.5 in (d). The labels are described both in Fig. 1 and in the text.

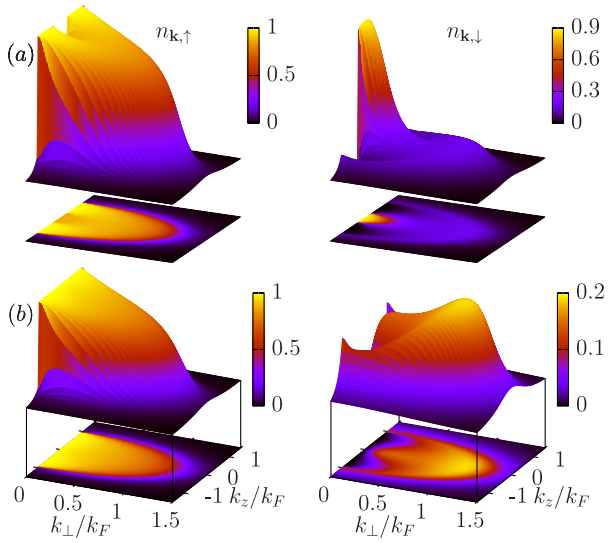

FIG. 3 (color online). Typical momentum distributions $n_{\mathbf{k},\sigma}$ are shown as a function of $k_\perp = \sqrt{k_x^2 + k_y^2}$ and k_z, where we set $P = 0.5$ and $1/(k_F a_s) = 0$, and vary the SOC parameter: (a) $\alpha = 0.275 k_F/m$ (for which $|\Delta| = 0.463\epsilon_F$, $\mu_+ = 0.550\epsilon_F$, and $\mu_- = 0.653\epsilon_F$), and (b) $\alpha = 0.350 k_F/m$ (for which $|\Delta| = 0.465\epsilon_F$, $\mu_+ = 0.427\epsilon_F$, and $\mu_- = 0.688\epsilon_F$), corresponding to GSF(II) and GSF(I) phases, respectively.

for which $E_{\mathbf{k},+}$ is always gapped. Depending on the number of zeros of $E_{\mathbf{k},-}$ (zero energy surfaces in $\mathbf{k}$ space), there are two topologically distinct GSF phases: GSF(I) where $E_{\mathbf{k},-}$ has two, and GSF(II) where $E_{\mathbf{k},-}$ has four zeros. The zeros of $E_{\mathbf{k},-}$ can be found by imposing the condition $E_{\mathbf{k},+}^2 E_{\mathbf{k},-}^2 = (\xi_{\mathbf{k},\uparrow}\xi_{\mathbf{k},\downarrow} + |\Delta|^2 - |S_\mathbf{k}|^2)^2 + 4|\Delta|^2|S_\mathbf{k}|^2 = 0$, indicating that both $|S_\mathbf{k}| = 0$ and $\xi_{\mathbf{k},\uparrow}\xi_{\mathbf{k},\downarrow} + |\Delta|^2 = 0$ needs to be satisfied.

For the Rashba-type SOC that we consider in this Letter, the zeros occur when $k_\perp = 0$ and at real k_z momenta, $k_{z,s}^2 = B_+ + s\sqrt{B_-^2 - 4m_\uparrow m_\downarrow |\Delta|^2}$, provided that $|\Delta|^2 < |B_-|^2/(4m_\uparrow m_\downarrow)$ for $B_+ \geq 0$, and $|\Delta|^2 < -\mu_\uparrow\mu_\downarrow$ for $B_+ < 0$. Here, $B_s = m_\uparrow\mu_\uparrow + s m_\downarrow\mu_\downarrow$. The topologically trivial superfluid phase corresponds to the case where both $E_{\mathbf{k},+}$ and $E_{\mathbf{k},-}$ have no zeros and are always gapped. The transition from GSF(II) to GSF(I) occurs when $|k_{z,-}| \to 0$, indicating a change in topology in the lowest quasiparticle band.

The topological transition discussed here is unique, because it involves an s-wave superfluid, and could be potentially observed through the measurement of the momentum distributions $n_{\mathbf{k},\sigma}$ of $\uparrow$ and $\downarrow$ fermions, both of which are readily available from Eqs. (3). For instance, we illustrate the typical $T = 0$ distribution of a GSF(II) phase in Fig. 3(a), and of a GSF(I) phase in Fig. 3(b). In these figures, we note that $n_{\mathbf{k},\sigma}$ is anisotropic in $\mathbf{k}$ space, which follows from the anisotropic structure of $E_{\mathbf{k},s}$. For $\mathbf{k}$-space regions where $k_\perp = 0$ and $k_{z,-} \leq |k_z| \leq k_{z,+}$, the corresponding distributions are exactly $n_{\mathbf{k},\uparrow} = 1$ and $n_{\mathbf{k},\downarrow} = 0$. Here, $k_{z,s}$ are approximately found to be $k_{z,-} = 0.30 k_F$ and $k_{z,+} = 1.01 k_F$ in Fig. 3(a), and $k_{z,-} = 0$ and $k_{z,+} = 0.97 k_F$ in Fig. 3(b), in perfect agreement with our analysis above. We also see that a major redistribution occurs for the minority species ($n_{\mathbf{k},\downarrow}$) at the GSF(II) to GSF(I) transition boundary, where the sharp peak that is present near the origin vanishes abruptly. Although this topological transition is quantum ($T = 0$) in nature, signatures of it should still be observed at finite T within the quantum critical region, where the $n_{\mathbf{k},\sigma}$ are smeared out due to thermal effects.

Conclusions.—In summary, we found that the SOC and population imbalance are counteracting, and that this competition always tends to stabilize the GSF phase against the PS. In contrast, while the SOC stabilizes the GSF phase against the N phase for low population imbalances, it destabilizes the GSF phase against the N phase for high population imbalances. In addition, we found topological quantum phase transitions associated with the appearance of momentum-space regions with zero quasiparticle energies, and studied their signatures in the momentum distribution. We hope that our work will motivate further research in this direction, since the SOC stabilizes the GSF phase for a very large parameter region, allowing for a possible realization of the GSF phase with cold atoms.

This work is supported by the Marie Curie International Reintegration (Grant No. FP7-PEOPLE-IRG-2010-268239), Scientific and Technological Research Council of Turkey (Career Grant No. TÜBİTAK-3501-110T839), and the Turkish Academy of Sciences (TÜBA-GEBİP).

[1] Y.-J. Lin *et al.*, Phys. Rev. Lett. **102**, 130401 (2009).
[2] Y.-J. Lin *et al.*, Nature (London) **471**, 83 (2011).
[3] M. Z. Hasan and C. L. Kane, Rev. Mod. Phys. **82**, 3045 (2010).
[4] M. Sato, Y. Takahashi, and S. Fujimoto, Phys. Rev. Lett. **103**, 020401 (2009).
[5] A. Kubasiak *et al.*, Europhys. Lett. **92**, 46004 (2010).
[6] S. Tewari *et al.*, New J. Phys. **13**, 065004 (2011); M. Gong *et al.*, arXiv:1105.1796.
[7] J. D. Sau *et al.*, Phys. Rev. B **83**, 140510 (2011).
[8] J. P. Vyasanakere and V. B. Shenoy, Phys. Rev. B **83**, 094515 (2011).
[9] J. P. Vyasanakere *et al.*, arXiv:1104.5633 [Phys. Rev. B (to be published)].
[10] Z.-Q. Yu and H. Zhai, arXiv:1105.2250.
[11] Hui Hu *et al.*, arXiv:1105.2488.
[12] S. Giorgini, L. P. Pitaevskii, and S. Stringari, Rev. Mod. Phys. **80**, 1215 (2008).
[13] M. W. Zwierlein *et al.*, Science **311**, 492 (2006); G. B. Partridge *et al.*, Science **311**, 503 (2006); Y. Shin *et al.*, Nature (London) **451**, 689 (2008); N. Navon *et al.*, Science **328**, 729 (2010).
[14] L. P. Gor'kov and E. I. Rashba, Phys. Rev. Lett. **87**, 037004 (2001).
[15] M. Iskin and C. A. R. Sá de Melo, Phys. Rev. Lett. **97**, 100404 (2006).
[16] L. He, M. Jin, and P. Zhuang, Phys. Rev. B **74**, 214516 (2006); Q. Chen *et al.*, Phys. Rev. A **74**, 063603 (2006).